

# ONLINE PARTITIONED LOCAL DEPTH FOR SEMI-SUPERVISED APPLICATIONS

JOHN D. FOLEY\* AND JUSTIN T. LEE\*

**Abstract.** We introduce an extension of the partitioned local depth (PaLD) algorithm that is adapted to online applications such as semi-supervised prediction. The new algorithm we present, online PaLD, is well-suited to situations where it is possible to pre-compute a cohesion network from a reference dataset. After  $O(n^3)$  steps to construct a queryable data structure, online PaLD can extend the cohesion network to a new data point in  $O(n^2)$  time. Our approach complements previous speed up approaches based on approximation and parallelism. For illustrations, we present applications to online anomaly detection and semi-supervised classification for health-care datasets.

**Key words.** online algorithms, semi-supervised learning, anomaly detection, networks, cohesion

**MSC codes.** 68W40, 68Q25, 62H30

**1. Introduction.** This article introduces an extension of the partitioned local depth (PaLD) algorithm to compute data cohesion adapted to online applications. PaLD excels at unsupervised, parameter-free clustering (highlighted in the Proceedings of the National Academy Sciences [5]) and is built on a probabilistic foundation with desirable theoretical properties [2, 5, 16]. The PaLD framework learns a network of communities in data that contains structural information beyond canonically induced clusters. PaLD has been applied to classification [14], data depth [7] and network science [3, 13]. The basis of the framework’s parameter-free robustness is relative comparisons among triples of data points, but this necessitates  $O(n^3)$  comparisons among data to compute cohesion exactly. Scaling to large datasets requires approximations [1].

Our extension, online PaLD, is adapted to applications where (i) a reference dataset is fixed and (ii) many individual test points may need to be compared to the reference network. After an upfront cost of making  $O(n^3)$  relative comparisons is paid, adding one more datum will entail  $O(n^2)$  further relative comparisons. This makes larger datasets accessible to exact analysis and complements previous work on scalability [1, 6, 14].

**Related Work.** The relatively new partitioned local depth (PaLD) framework [4, 5] has been developed theoretically [2, 5, 16] and practically in terms of scalability [1, 6, 14] and applications to data [3, 5, 7, 12, 13]. The basic theory is developed in the seminal work [5] which is extended by the generalized PaLD approach [2] to manage variation and uncertainty. In [16], the foundations are reconsidered, including analysis of probabilistic weights on data and consistency with combining weights. Applications of PaLD include biological [5, 7, 12, 13] and social settings [2, 3, 5].

Two directions to develop the scalability of PaLD include approximation techniques [1] and computer science approaches to address how the data is processed [6, 14]. The Partitioned Nearest Neighbors Local Depth (PaNNLD) algorithm [1] computes an approximation of cohesion by analyzing the  $k$ -nearest neighbor digraph. By employing coin flips to resolve relatively low impact triplet comparisons, a principled approximation (with bounded error) is obtained. Work to improve data processing includes a simple Python implementation adapted to GPU processing [14] and analysis to design sequential and shared-memory parallel algorithms for PaLD [6].

---

\*Metron, Inc., 1818 Library St., # 600, Reston, VA (foley@metsci.com, leej@metsci.com)

**Summary of Contribution.** After  $O(n^3)$  steps to construct a queryable data structure, online PaLD can extend the cohesion network to a new test point in  $O(n^2)$  time. Specifically, the new algorithm computes the new neighborhood of the test datum in the extended cohesion network as well as an updated strong cohesion threshold in  $O(n^2)$  steps. These determinations are exact, implementation is relatively simple, and a basic validation of the speedup is in line with complexity analysis. See Table 1 below and Section 2 for further details, including a description of our prototype implementation in subsection 2.3.

TABLE 1

Mean run times for baseline partition local depth (PaLD) algorithm on  $n + 1$  data points vs. online PaLD to compute neighborhood on  $n + 1$ -st point  $t$ , averaged over 100 sample runs.

$n$	Base PaLD (sec)	Online PaLD (sec)
7	2e-3	1.6e-4
15	3e-3	2.3e-4
239	0.93	0.032
499	6.2	0.17
787	28.4	0.434
999	64.1	0.844
1999	612	4.15

Though fully caching contributions to cohesion would require up to  $O(n^3)$  memory, under mild assumptions, the memory need for online applications can be reduced to  $O(n^2)$ . Moreover, the required memory is based on the outcomes of relative comparisons and is independent of data dimensionality.

Online PaLD opens the potential for applications to online anomaly detection and semi-supervised prediction for moderately sized data sets without the need for approximation techniques [1] or more complex implementations [6, 14]. For instance, the THINGS initiative [11] has developed 1,854 (highly-curated) concepts as a bridge between research in human cognition and artificial intelligence (see also Section 4 below). Based on Table 1, online PaLD would be suitable to build an online tool to relate test data to THINGS concepts. To explore applications to anomaly detection and prediction, experimentation across datasets and algorithmic details will be needed. Since online PaLD is relatively simple to implement, researchers can readily extend their environment include online PaLD to accelerate testing (see subsection 3.2 for related discussion). For big data, the presented approach might provide a complementary means to reduce algorithmic runtime, but this would require future work to hybridize with approximation approaches [1].

**Organization of the paper.** Our main results and algorithm design are in Section 2 including a basic validation of the speed up (see Table 1). Applications to health-care data appear in Section 3 and discussion follows in Section 4.

**2. A query formulation of PaLD.** The novel partitioned local depth (PaLD) algorithm adapts a dissimilarity measure [5]. PaLD’s intrinsic basis on relative comparisons among triples of data aids its robustness but results in an algorithm with  $O(n^3)$  computational steps. However, after an upfront cost of  $O(n^3)$  computational steps is paid, considering one more datum entails  $O(n^2)$  further relative comparisons. For a setting in which (i) a reference dataset is fixed and (ii) many individual test points may need to be compared to reference data (see, e.g., [14]), it would be advantageous to pay the upfront cost to analyze the reference dataset, once and for all, and then pay the marginal to cost reason about test points, as needed. See Section 3 for example applications to health-care datasets.

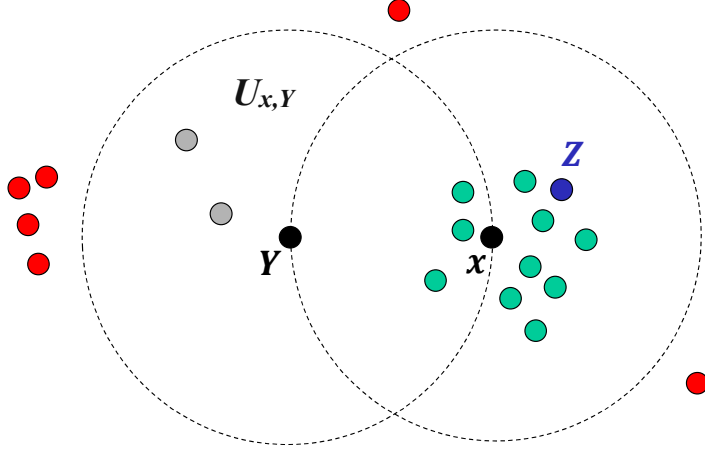


FIG. 1. Example local focus for a fixed point  $x$  and a random point  $Y$  in two dimensions. Red points are outside the focus. Those in green (and  $Z$  in blue) are in the focus and closer to  $x$  while those in grey are closer to  $Y$ . Figure from [2].

Here we realize this idea as an explicit algorithm. After reviewing PaLD, we present our new query algorithm, made simpler by assuming that the dissimilarity measure to be adapted is symmetric.

**2.1. Review of PaLD.** The partitioned local depth (PaLD) algorithm reasons over a finite set  $S$  of data with a pairwise notion of dissimilarity or distance  $d(x, y)$ . For any data pair  $(x, y)$ , the relevant local data is the set of points  $z$  within  $d(x, y)$  of  $x$  or  $y$ :

$$(2.1) \quad U_{x,y} \stackrel{\text{def}}{=} \{z \in S \mid d(z, x) \leq d(y, x) \text{ or } d(z, y) \leq d(x, y)\}.$$

called the *local focus* of the pair  $(x, y)$ ; compare Figure 1. *Cohesion* is a probabilistic quantity obtained from an intuitive sampling process: select  $Y \neq x$  uniformly and then a uniform  $Z \in U_{x,Y}$ . Then, define the cohesion of  $w$  to  $x$  as:

$$(2.2) \quad c_{x,w} \stackrel{\text{def}}{=} P(Z = w, d(Z, x) < d(Z, Y)) + \frac{1}{2} P(Z = w, d(Z, x) = d(Z, Y)).$$

This sampling process is illustrated in Figure 1: once  $Y \neq x$  is selected (black points), a uniform  $Z \in U_{x,Y}$  (blue) is selected. In Figure 1, red points are outside the local focus and thus, not sampled. Here the blue point  $w$ , any green point, and  $x$  itself are potential elements  $Z$  of  $U_{x,Y}$  such that  $d(Z, x) < d(Z, Y)$  but only  $Z = w$  contributes to the cohesion of  $w$  to  $x$ :  $c_{x,w}$ . For additional discussion and applications, including the relationship to data depth as well as considerations for parameter-free clustering and near-neighbors, see [5]. Theoretical properties of the framework are covered in [2, 5, 16].

**Computing cohesion.** As various  $Y \neq x$  are sampled, further contributions to the cohesion of  $w$  to  $x$  accumulate. Explicitly, if  $|S| = n$ , then:

$$(2.3) \quad c_{x,w} = \frac{1}{n-1} \sum_{y \in S, y \neq x} \frac{I(w \in U_{x,y})}{|U_{x,y}|} I(w, x, y)$$

for:

$$(2.4) \quad I(w, x, y) = \begin{cases} 1, & \text{if } d(w, x) < d(w, y) \\ 1/2, & \text{if } d(w, x) = d(w, y) \\ 0, & \text{otherwise} \end{cases}.$$

where  $1/(n-1)$  is the sampling weight for  $Y \neq x$ ,  $1/|U_{x,y}|$  is the sampling weight for  $Z \in U_{x,y}$  and the indicator function  $I(w, x, y)$  divides support, as determined by the definition of the cohesion of  $w$  to  $x$  (2.2). In the more general settings (e.g., when quantifying data uncertainty), the sampling weight for  $Z \in U_{x,y}$  can be abstracted to the concept of *local relevance* and the indicator is captured by *support division* within the generalized PaLD framework; see [2] for further discussion and more general notation.

---

**Algorithm 2.1** PaLD: reference implementation to compute cohesion (2.2)

---

Given  $D(S, S) = \{d(x, y)\}_{x,y=1}^n$ , initialize  $C \leftarrow \{0\}_{x,y=1}^n$ .

**for**  $x = 1$  to  $n$  **do**

**for**  $y = 1$  to  $n$  such that  $y \neq x$  **do**

$U_{x,y} \leftarrow \emptyset$

**for**  $w = 1$  to  $n$  **do**

**if**  $d(w, x) \leq d(y, x)$  or  $d(w, y) \leq d(x, y)$  **then**

$U_{x,y} \leftarrow U_{x,y} \cup \{w\}$

**for**  $w \in U_{x,y}$  **do**

$C_{x,w} \leftarrow C_{x,w} + \frac{I(w,x,y)}{|U_{x,y}|}$

$C \leftarrow C/(n-1)$

**return**  $C$

---

Based on the above, a reference implementation for PaLD to compute a cohesion matrix from  $O(n^3)$  relative comparisons is given as Algorithm 2.1. This approach is only lightly optimized in PaLD's open-source R package [15] (e.g., by applying vectorization strategies). See [1] for approximation techniques and [6, 14] for examples of parallel processing approaches.

The *cohesion network*  $G_S$  is the weighted, undirected graph with node set  $S$  and edge weights:

$$(2.5) \quad w_{x,y} \stackrel{\text{def}}{=} \min(c_{x,y}, c_{y,x}).$$

One can consider these  $w_{x,y}$  as being a locally adapted (and probabilistically normalized) version of  $d(x, y)$ <sup>1</sup>: if  $w_{x,y}$  is higher, then the pair  $(x, y)$  is more closely tied, in a locally adapted, relative sense.

Under the mild assumption that  $d(z, z) < d(z, y)$  for all distinct  $z, y \in S$ , there is a natural probabilistic threshold:

$$(2.6) \quad \tau = \frac{1}{2n} \sum_{x \in S} c_{x,x}$$

---

<sup>1</sup>The self-cohesion values  $c_{x,x}$  can be interpreted as a localized measure of depth in the sense that the explicit formula (2.3) indicates that large self-cohesion corresponds to membership in relatively small local foci  $U_{x,y}$ , due to being relatively similar to local data.

that provides a canonical and useful point of reference for these probabilistically derived quantities; see [5] for the general definition and further discussion. A link in  $G_S$  is strong if and only if  $w_{x,y} \geq \tau(S, d)$ <sup>2</sup>. Thus, by locally adapting dissimilarity, a natural threshold straightforwardly determines which  $y$  are “near”  $x$ :  $y$  such that  $w_{x,y} \geq \tau(S, d)$ .

For our motivating setting—in which  $S$  is a fixed reference dataset and there is an individual test point  $t$  for online analysis—if  $w_{t,y} < \tau(S, d)$  for all  $y$  in the reference set  $S$ , then  $t$  can be considered an outlier<sup>3</sup>. Likewise,  $y$  with  $w_{t,y} \geq \tau(S, d)$  are natural reference points to compare to the test point, e.g., for semi-supervised classification [14] similar to k-nearest neighbor approaches.

**2.2. A query formulation of PaLD to add a single datum.** The explicit formula for cohesion (2.3) exposes that three quantities determine its value: set membership in the local foci  $U_{x,y}$ , the cardinalities  $|U_{x,y}|$ , and the indicator function values  $I(w, x, y)$ . With this in mind, let us consider adding a datum  $t$  to  $S$  so that  $T := S \cup \{t\}$  constitutes the extended dataset of interest.

We then see that the cohesion of  $w$  to  $t$  is given by:

$$(2.7) \quad c_{t,w}^T = \frac{1}{n} \sum_{y \in S} \frac{I(w \in U_{t,y})}{|U_{t,y}^T|} I(w, t, y)$$

where we employ superscripts to make the use of the extended dataset  $T = S \cup \{t\}$  explicit when referring to  $U_{t,y}^T$  and  $c_{t,w}^T$ , as opposed to the previous, implicit notation (2.3) that assumed the reference dataset  $S$ . Here it is clear that  $c_{t,w}^T$  depends only on the relative comparisons that involve the test point  $t$ . That is, if we assign the index  $(n+1)$  to  $t$ , then a reference implementation to compute cohesion to  $t$  is given as **Algorithm 2.2**. Here the vector of dissimilarities  $D(t, S)$  can be computed in  $O(n)$  steps and this computation includes self-cohesion for  $t$ —i.e., the cohesion of  $t$  to  $t$ .

Conceptually, the cohesion to  $t$  always involves  $t$  and—since  $t$  is fixed—at most  $O(n^2)$  comparisons (based on  $O(n)$  dissimilarities). That is, in [Figure 1](#),  $x = t$  is always present when determining  $c_{t,w}^T$ , including when determining  $U_{t,y}^T$ .

---

**Algorithm 2.2** CohesionToNew: compute cohesion to a new test point  $C_{t,-}^T$

---

Given  $D(t, S) = \{d(t, y), d(y, t)\}_{y=1}^n$ , initialize  $C_{t,-}^T \leftarrow \{0\}_{y=1}^n$ .

```

for  $y = 1$  to  $n$  do
  for  $w = 1$  to  $n+1$  do
     $U_{t,y}^T \leftarrow \emptyset$ 
    if  $d(w, t) \leq d(y, t)$  or  $d(w, y) \leq d(t, y)$  then
       $U_{t,y}^T \leftarrow U_{t,y}^T \cup \{w\}$ 
    for  $w \in U_{x,y}^T$  do
       $C_{t,w}^T \leftarrow C_{t,w}^T + \frac{I(w, t, y)}{|U_{x,y}^T|}$ 
   $C_{t,-}^T \leftarrow C_{t,-}^T / n$ 
return  $C_{t,-}^T$ 

```

---

<sup>2</sup>Such strong links form a subnetwork of  $G_S$  called the cluster network  $G_S^*$ , whose components determine a data-driven partitioning of  $S$  into clusters without tuning parameters. Strong performance relative to clustering benchmarks was shown in [5].

<sup>3</sup>For comparison, when PaLD is applied to parameter-free clustering [5], any point with no strong links forms its own cluster of size one.

Asymmetrically, the cohesion of  $t$  to  $w \neq t$  is given by:

$$(2.8) \quad c_{w,t}^T = \frac{1}{n} \sum_{y \in S} \frac{I(t \in U_{w,y})}{|U_{w,y}^T|} I(t, w, y).$$

where we emphasize that  $U_{w,y}^T$  depends on the extended dataset  $T = S \cup \{t\}$ . Exact computation of  $c_{w,t}^T$  is possible in  $O(n^2)$  steps, if  $U_{w,y}^S$  are provided as input. Since  $U_{w,y}^S$  and  $\{t\}$  are disjoint for distinct  $w, y \in S$ , either  $U_{w,y}^T = U_{w,y}^S$  or  $U_{w,y}^T = U_{w,y}^S \cup \{t\}$ . That is,  $|U_{w,y}^T|$  is at most one greater than  $|U_{w,y}^S|$  and we have a reference implementation to compute cohesion of  $t$  to  $w$  in  $S$  given as [Algorithm 2.3](#).

Intuitively, even though cohesion from  $t$  always involves  $t$ , knowledge of  $|U_{w,y}^T|$  is needed to appropriately weight the contributions from  $t$  to  $c_{w,t}^T$ . That is, in [Figure 1](#),  $Z = t$  is always present, but  $t$  is not involved in the determining the red points based on the pair  $(Y, w = x)$ . Even though  $t$  is fixed, determination regarding these four parties are needed. On the other hand, if the separation of red points from the grey, green and black points in  $U_{w,y}^S$  was determined in advance, then *any*  $t$  can be tested against the pair  $(Y, w = x)$ : first determine if  $t \in U_{w,y}^T$  and second, if  $t \in U_{w,y}^T$ , then determine if  $t$  is closer to  $w$  than  $Y$ .

---

**Algorithm 2.3** CohesionToS: compute cohesion from a new test point  $C_{-,t}^T$

---

Given  $D(t, S) = \{d(t, y), d(y, t)\}_{y=1}^n$ ,  $D(S, S) = \{d(x, y)\}_{x,y=1}^n$   
 and  $U(S, S) = \{U_{x,y}\}_{x,y=1}^n$ , initialize  $C_{-,t}^T \leftarrow \{0\}_{y=1}^n$ .  
**for**  $y = 1$  to  $n$  **do**  
   **for**  $w = 1$  to  $n$  **do**  
      $U_{t,y}^T \leftarrow U_{t,y}^S$   
     **if**  $d(t, w) \leq d(t, y)$  or  $d(t, y) \leq d(w, y)$  **then**  
        $U_{w,y}^T \leftarrow U_{w,y}^T \cup \{t\}$   
     **for**  $w \in U_{x,y}^T$  **do**  
        $C_{w,t}^T \leftarrow C_{w,t}^T + \frac{I(t, w, y)}{|U_{w,y}^T|}$   
      $C_{-,t}^T \leftarrow C_{-,t}^T / n$   
**return**  $C_{-,t}^T$

---

The reference implementations given above show that:

- an  $O(n^2)$  query algorithm for cohesion is, in general, possible and
- the memory required is at most  $O(n^3)$  to maintain: (i)  $O(n^2)$  local foci  $U_{x,y}$ , each of which requires no more than  $O(n)$  memory; and (ii) support indicators  $I(w, x, y)$ .

In particular, it is possible to iteratively build up the local foci  $U_{x,y}$  and dissimilarity data  $d(x, y)$  needed to compute cohesion. Within the generalized PaLD framework [\[2\]](#), the contributions to cohesion still require at most  $O(n^3)$  memory to maintain. Moreover, for practical applications, sparse representations of the contributions to cohesion can help control the growth of memory required and, if approximations are acceptable (see [\[1\]](#)), memory consumption might be further limited. However, detailed consideration of more general settings and the potential for principled approximation techniques are beyond the scope of the present article<sup>4</sup>.

---

<sup>4</sup>For brief discussion of the complexity challenges of maintaining the full cohesion network, see [subsection A.3](#).

We now turn to practical considerations for the much simpler situation where a reference data set  $S$  is fixed and test points  $t$  are considered one at a time. As we illustrate in [Section 3](#) below, these assumptions support using labeled  $S$  for semi-supervised classification and unlabeled  $S$  for online anomaly detection.

**Practical considerations and the natural threshold.** For these purposes, we make the simplifying assumptions that:

$$(2.9) \quad d(y, z) = d(z, y) \text{ and } d(z, z) < d(z, y) \text{ for all distinct } y, z \in T.$$

A notable practical consideration is determining the natural threshold  $\tau(T, d)$  for cohesion—e.g., if the test point  $t$  has  $w_{t,y} < \tau(T, d)$  for all  $y \in S$ , then  $t$  might be considered an outlier. Ideally, we would start from an exact computation of  $\tau(T, d)$  and introduce any practical approximations from there. After giving an approach to determine  $\tau(T, d)$  exactly, we describe how to precompute quantities for the reference set  $S$ , at an upfront cost of  $O(n^3)$ , and compute the strong neighborhood of  $t$  in  $O(n^2)$  steps during the online stage of the approach. By caching the cardinalities of local foci for the reference data  $S$ , the memory requirements are at most  $O(n^2 + nd)$ , where  $d$  is the data dimensionality.

The observation that  $\tau(S, d)$  relates directly to the size of local foci via:

$$(2.10) \quad 2n(n-1)\tau(S, d) = \sum_{x \in S} \sum_{y \in S, y \neq x} \frac{1}{|U_{x,y}^S|}$$

enables marginal analysis of the impact of adding a single datum  $t$ . Under our simplifying assumptions, this leads to an attractive marginal formula for  $\tau(T, d)$ :

$$(2.11) \quad \tau(T, d) = \tau(S, d) \frac{n-1}{n+1} + \frac{c_{t,t}^T}{n+1} - \frac{1}{2n(n+1)} \sum_{x \in S} \sum_{y \in S, y \neq x} \frac{I(t \in U_{x,y}^T)}{(|U_{x,y}^S| + 1)|U_{x,y}^S|}$$

in which we can view the right most term

$$(2.12) \quad \varepsilon(T, d) \stackrel{\text{def}}{=} \frac{1}{2n(n+1)} \sum_{x \in S} \sum_{y \in S, y \neq x} \frac{I(t \in U_{x,y}^T)}{(|U_{x,y}^S| + 1)|U_{x,y}^S|}$$

as a correction for those local foci that  $t$  is added when extending  $S$  to  $T$ ; see [subsection A.1](#) for derivation details.

**Example.** To get a more “hands on” feel for the marginal formula (2.11), consider  $S = \{z, w\}$ . Then,

$$(2.13) \quad 2n(n-1)\tau(S, d) = \sum_{x \in S} \sum_{y \in S, y \neq x} \frac{1}{|U_{x,y}^S|} = \frac{1}{|U_{z,w}^S|} + \frac{1}{|U_{w,z}^S|} = \frac{1}{2} + \frac{1}{2}$$

where  $n = 2$ .

When extending to  $T = \{z, w, t\}$ , if both  $d(z, t)$  and  $d(w, t)$  and are greater than  $d(z, w)$ , then (noting our assumptions (2.9)), the relatively distant test point  $t$  will not be added to any local focus. This implies:

$$\begin{aligned} 2(n+1)n\tau(T, d) &= \sum_{x \in T} \sum_{y \in T, y \neq x} \frac{1}{|U_{x,y}^T|} = \frac{1}{|U_{t,w}^T|} + \frac{1}{|U_{w,t}^T|} + \sum_{x \in S} \sum_{y \in T, y \neq x} \frac{1}{|U_{x,y}^T|} \\ &= \frac{1}{|U_{t,w}^T|} + \frac{1}{|U_{w,t}^T|} + \frac{1}{|U_{w,z}^T|} + \frac{1}{|U_{t,z}^T|} + \sum_{x \in S} \sum_{y \in S, y \neq x} \frac{1}{|U_{x,y}^T|} \\ (2.14) \quad &= 2nc_{t,t}^T + 2n(n-1)\tau(S, d) \end{aligned}$$

where the bottom equality follows from symmetry, the fact that local foci do not increase in size for distinct  $x, y \in S$ , and the previous formula. Thus, to dividing by  $2(n+1)n$ , we have:

$$(2.15) \quad \tau(T, d) = \tau(S, d) \frac{n-1}{n+1} + \frac{c_{t,t}^T}{n+1}$$

with  $\varepsilon(T, d) = 0$ . In this case,  $t$  was relatively distant and did not join any existing local foci.

If  $d(z, t) < d(z, w) < d(w, t)$ , then:

$$(2.16) \quad \begin{aligned} 2(n+1)n\tau(T, d) &= \frac{1}{|U_{t,w}^T|} + \frac{1}{|U_{w,t}^T|} + \frac{1}{|U_{w,z}^T|} + \frac{1}{|U_{t,z}^T|} + \sum_{x \in S} \sum_{y \in S, y \neq x} \frac{1}{|U_{x,y}^T|} \\ &= 2nc_{t,t}^T + \frac{1}{|U_{z,w}^T|} + \frac{1}{|U_{w,z}^T|} \\ &= 2nc_{t,t}^T + 2n(n-1)\tau(S, d) - \sum_{x \in S} \sum_{y \in S, y \neq x} \frac{1}{(|U_{x,y}^T| |U_{x,y}^S|)} \end{aligned}$$

where the bottom equality includes a correction term  $\varepsilon(T, d) > 0$  since  $U_{x,y}^S = U_{y,x}^S$  must be increased when extending  $S$  to  $T$ . Thus, we have a correction term for all (two) local foci for distinct  $x, y \in S$  in this case, so that:

$$(2.17) \quad \tau(T, d) = \tau(S, d) \frac{n-1}{n+1} + \frac{c_{t,t}^T}{n+1} - \frac{1}{2n(n+1)} \sum_{x \in S} \sum_{y \in S, y \neq x} \frac{1}{(|U_{x,y}^S| + 1) |U_{x,y}^T|}.$$

For more general  $n$ , correction terms are introduced based on the indicator  $I(t \in U_{x,y}^T)$ .

□

---

**Algorithm 2.4** PaLDSymCache: compute data to query strong neighborhoods

---

Given  $D(S < S) = \{d(x, y)\}_{y>x=1}^n$ , initialize  $V \leftarrow \{0\}_{y=1}^n$ ,  $\tau(S) \leftarrow 0$ .

**for**  $x = 1$  to  $n-1$  **do**

**for**  $y = x+1$  to  $n$  **do**

**for**  $w = 1$  to  $n$  **do**

**if**  $d(w, x) \leq d(w, y)$  or  $d(w, y) \leq d(x, y)$  **then**

$V_{x,y} \leftarrow V_{x,y} + 1$

$\tau(S) \leftarrow \tau(S) + \frac{2}{V_{x,y}}$

$\tau(S) \leftarrow \frac{\tau(S)}{2n(n-1)}$

**return**  $V, \tau(S)$

---

We conclude this section with our approach to implementing online PaLD by storing information for queries. We employ a new notation  $V_{x,y} = V_{x,y}^S := |U_{x,y}^S|$  and  $V_{x,y}^T := |U_{x,y}^T|$ , for brevity, as well as our notations cohesion (2.3), the strong threshold (2.10), and the correction term  $\varepsilon(T, d)$  (2.12).

After precomputation with the reference data  $S$ , the strong neighborhood of any new test point  $t$  is computed in  $O(n^2)$  steps:

1. Cache the sizes of local foci  $V_{x,y}$ , as when computing  $C$ , and sum contributions to  $\tau(S, d)$ . This incurs an upfront cost of  $O(n^3)$  (Algorithm 2.4).

2. Compute the cohesion of  $w$  to  $t$  in  $O(n^2)$  steps (Algorithm 2.2), which does not require cached data as discussed above.
3. Compute the cohesion of  $t$  to  $w \neq t$  in  $O(n^2)$  steps using the sizes of the local foci  $V_{x,y}$  as input and summing corrections due to the specific local foci whose sizes increase (Algorithm 2.5). This modifies Algorithm 2.3 to use the cached cardinalities from Step 1 and compute  $\varepsilon(T, d)$ .
4. Update the strong threshold via (2.11).
5. Determine the strong neighborhood of  $w_{t,y} \geq \tau(T, d)$  in  $O(n)$  steps by checking if the minimum of  $c_{x,y}$  and  $c_{y,x}$  (computed in steps 2 and 3) meet or exceed  $\tau(T, d)$  (computed in step 4).

---

**Algorithm 2.5** QueryCohesionToS: compute cohesion from a new test point  $C_{-,t}^T$ 


---

Given  $D(S < t) = \{d(y, t)\}_{y=1}^n$ ,  $D(S < S) = \{d(x, y)\}_{y>x=1}^n$  and

$V = \{V_{x,y}\}_{y>x=1}^n$ , initialize  $C_{-,t}^T \leftarrow \{0\}_{y=1}^n$   $\varepsilon(T, d) \leftarrow 0$

**for**  $y = 1$  to  $n$  **do**

$V_{y,y}^T \leftarrow 2$

**for**  $w = 1$  to  $y - 1$  **do**

$V_{w,y}^T \leftarrow V_{w,y}^S$

**if**  $d(t, w) \leq d(y, w)$  or  $d(t, y) \leq d(w, y)$  **then**

$V_{w,y}^T \leftarrow V_{w,y}^T + 1$

$\varepsilon(T, d) \leftarrow \varepsilon(T, d) + \frac{1}{V_{w,y}^T(V_{w,y}^T - 1)}$

**for**  $w = 1$  to  $n$  **do**

$C_{w,t}^T \leftarrow C_{w,t}^T + \frac{I(t,w,y)}{V_{w,y}^T}$

$C_{-,t}^T \leftarrow C_{-,t}^T / n$

$\varepsilon(T, d) \leftarrow \varepsilon(T, d) / (n(n + 1))$

**return**  $C_{-,t}^T$ ,  $\varepsilon(T, d)$

---

**2.3. Experimental validation of speed up.** Standard PaLD implementations [15] require  $O(n^3)$  comparison steps to analyze a set of  $n$  data points. For online PaLD, a second pass of  $O(n^2)$  comparisons to reference data is needed each time a new datum is considered. The first, unsupervised, pass discovers communities intrinsic to the reference dataset. The second pass associates a new data point, called a test point, to the original communities in the reference data. When the reference data is labeled, this second pass can be considered a form of semi-supervised learning: the reference labels provide information about test points to predict their labels.

This type of analysis is similar to the k-nearest neighbors (knn) classification framework where a new test point is assigned the label that represents a best guess based on the labels of its  $k$  closest neighbors. Ideally, PaLD partitions reference data points into communities such that each community has an intrinsic label. A new test point can then be assigned the same label as the existing community that online PaLD associates it with. Figure 2 provides an example of this semi-supervised use case where online PaLD was used to visualize the decision boundary between two clusters of data. In Figure 2, white areas capture potential test data that might not naturally fall into either class (see [14] for comparison and further discussion) and could be considered outliers relative to the labeled reference data.

**Test Implementation.** To validate the approach from subsection 2.2, we implemented online PaLD in Python. As a baseline, we implemented a lightly vectorized

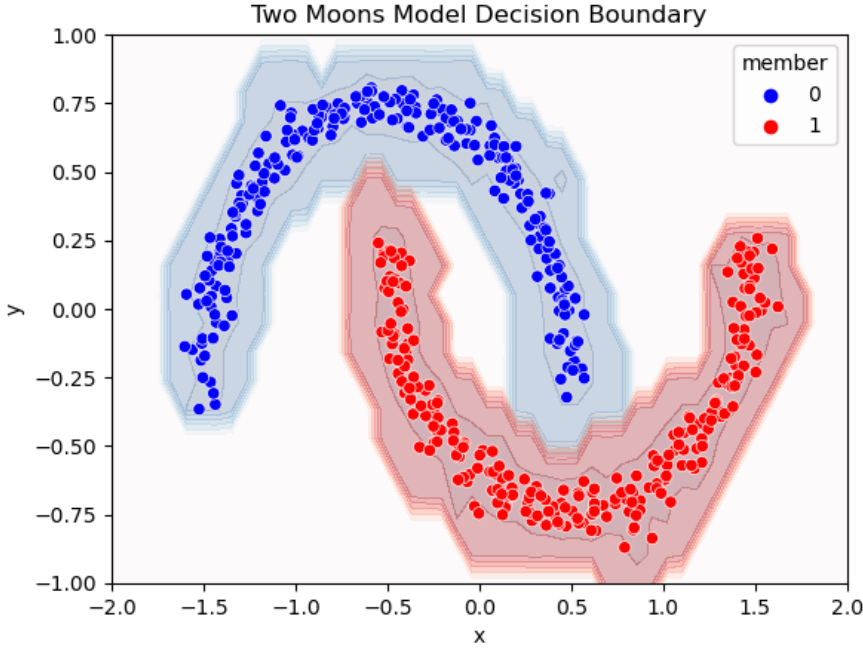


FIG. 2. *Visualization of the decision boundary between two reference classes or clusters.*

version of [Algorithm 2.1](#)—similar to publicly available R package (<https://CRAN.R-project.org/package=pald>) [15] with `numpy` standing in as the vector library. To build a queryable data structure, we implemented [Algorithm 2.2](#) through [Algorithm 2.5](#) as a Python interface called `CohesionDB`. For example, constructing `CohesionDB` pays the upfront cost of recording the cardinality of the local foci between every pair of samples found in the reference data ([Algorithm 2.4](#)). In particular, this supports lazy calculation of all  $c_{x,w}^S$  for  $x, w \in S$  to get a sense of the communities intrinsic to the reference data  $S$  in addition to online computation  $c_{x,t}^T$  and  $c_{t,x}^T$  for a test point  $t$ . Results for lazy computation are reported in [Table 2](#) below.

**Results.** We used data from [5] and clustering benchmarks [8, 17] for speed up validation. This corresponds to a contrived situation in which a single test point is held out for “testing”, but keeps our focus on timing. Speed tests were performed on a Dell laptop with an Intel(R) Core(TM) i7-10875H CPU with 64 GB of RAM. Our evaluation pipeline consisted of dataset management through the `DVC` package and performance tabulation using `mlflow`. In the next section, we present initial applications of the approach to health-care data.

We compared our online PaLD implementation to a straightforward Python implementation for datasets of different sizes and captured the processing time along various stages. Seven base datasets  $T$  of size  $n$  were split into a reference set  $S$  of size  $n - 1$  and a single test datum  $t$ . We measured 100 iterations of the following actions: (1) loading the data into an internal structure consisting of nested dictionaries for fast look-up times, (2) querying for the local foci and its cardinality between two points, (3) calculating the cohesion between reference data, (4) calculating the cohesion to a new test point, (5) calculating the cohesion from a new test point, and (6) building the cohesion matrix.

TABLE 2

Mean run times for baseline partition local depth (PaLD) algorithm on  $n$  reference data points vs. lazy computation of the cohesion network, averaged over 100 sample runs.

$n$	Base PaLD (sec)	Online PaLD (sec)			
		Network	Loading	Lazy Network	Total
7	2e-3	3.9e-4	7.6e-4	1.1e-3	
15	3e-3	2e-3	4e-3	6e-3	
239	0.97	0.64	1.3	1.9	
499	5.9	4.6	7.8	12.4	
787	26.6	13.8	23.5	37.3	
999	64.1	28.0	45.0	72.9	
1999	612	207	290	497	

Basic runtime comparisons for analyzing a test point  $t$  are recorded in [Table 1](#). For a single test point, online PaLD is faster. In line with complexity analysis, the magnitude of the speedup is roughly scaling with  $|S| = n$ .

Comparisons of runtime for computing the cohesion network for the reference data  $S$  are given in [Table 2](#). For small  $S$ , the overhead cost of pre-compute and creating the internal data representation (Loading step) leads to slowdown. However, the lazy approach to compute the cohesion network for  $S$  may provide speedup opportunities for larger  $S$  in terms of total time to compute reference communities. In any case, if online computation is expected later (which requires the Loading step), it is reasonable to use cached data (from the Loading step) to display and analyze the reference network. The online Lazy Network step to build the cohesion network is trending to be faster than the baseline Network step, so it makes sense to take advantage of data cached during Loading. As  $n$  increases toward  $10^5$ , the Total online runtime may even be preferred but detailed study is beyond our present scope.

Overall, these experimental results exhibit runtimes in line with complexity analysis. In practice, Online PaLD makes online applications with  $n = 10^5$  accessible with straightforward, if lengthy, training (less than one day) and acceptable query times (less than two minutes). Many interesting health-care data sets fall into this regime and we consider example applications in the next section.

**3. Applications.** In this section, we present two application areas as illustrations of online PaLD: online anomaly detection and semi-supervised prediction. Our illustrations provide starting points to help stimulate further study and indicate how online PaLD can speed exploration.

For online anomaly detection, online PaLD is a novel approach. At the time of this writing, we are not aware of example applications of PaLD to anomaly detection in print. The examples presented below suggest that while PaLD-based anomaly detection is conceptually similar to  $k$ -nearest neighbors, it may perform quite differently.

For semi-supervised prediction, we give an example where the number of reference samples is smaller (low  $n$ ) than the dimensionality of each sample (high  $d$ ). Online PaLD is adapted to high  $d$ , but moderate  $n$ , applications since (i) PaLD's basis on relative comparisons may help mitigate the curse of dimensionality (cf. [\[5, Fig. 8\]](#)) and (ii) its memory requirements collapse the dimensionality of reference data. That is, the memory needed for online PaLD is dominated by storing the reference data  $S$  at  $O(n \times d)$  cost for  $S$  with sufficiently high dimensionality<sup>5</sup>.

Throughout, we employ health-care datasets, which are often not massive and

<sup>5</sup>Moreover, reference data can be accessed from disk as opposed to being cached in RAM.

can present challenges that may warrant novel data science approaches. For example, the distribution normal subject data may have different features than anomalous or pathological populations. Within the population of subjects with known pathology, different sub-populations exhibit characteristic features to distinguish modes of pathology but have low frequency within the general population.

**3.1. Online anomaly detection.** A typical finding for diverse anomaly detection benchmarks is that that anomaly detection performance varies significantly by application [9]. In practice, experimentation with a variety of anomaly detection algorithms may help tune performance to a specific application. PaLD-based anomaly detection is conceptually similar to  $k$ -nearest neighbors (knn), including its suitability for data with high dimensionality. If PaLD reproduces the performance of knn, then its value as a new candidate algorithm may be limited. On the other hand, if PaLD behaves differently than knn, then it provides a conceptually similar candidate algorithm. In these initial experiments, we see that online PaLD may perform quite differently from knn. Moreover, online PaLD is potentially a good complement to the suite of 14 unsupervised algorithms considered in [9], especially for challengingly anomaly detection benchmarks, which may warrant broader exploration of candidates.

**Experimental design.** As a simple test of online PaLD’s potential for online anomaly detection, we compare performance to  $k$ -nearest neighbors (knn) for eight anomaly detection benchmarks for health-care data. Considering benchmarks from ADBench [9], these datasets have sample counts less than 3000 (min: 80, max: 2114), which supports online anomaly detection within seconds<sup>6</sup>. Rather than setting specific thresholds for detection, we focus area under curve (AUC) metrics for the receiving operator characteristic (ROC) and precision recall (PR) curves, as in ADBench [9].

There are choices to derive a test statistic from cohesion (see [14], for comparison, in the context of classification). For simplicity, our test statistic is the maximal  $w_{x,t}$  (2.5) value where  $t$  is the datum being tested and  $x$  ranges of normal (non-anomaly) reference values  $N$ <sup>7</sup>. That is, our online test statistic for  $t$  is

$$(3.1) \quad a(t) \stackrel{\text{def}}{=} \max_{x \in N \subset S} w_{x,t}^N$$

where  $N \subset S$  is the set of non-anomaly values within the reference data  $S$  and lower values  $a(t)$  indicate that  $t$  is more likely to be an anomaly. In practice, this means that known anomalies have been removed from a normal data to the degree possible. In terms of parameter-free clustering [5], a value of  $a(t)$  less than the natural threshold would be deemed its own cluster as compared with normal reference values  $N$ . Our knn parameters follow ADBench [9] where the default number of near neighbors is 5. To facilitate comparisons with ADBench, we use its setup to define a new candidate algorithm based on  $a(t)$  (3.1) so that the details of training and testing splits follow ADBench conventions.

**Results.** To indicate the relative difficulty of these anomaly detection problems, we report the metric for the highest performing unsupervised algorithm considered in [9]. Our results are summarized in Table 3 and suggest that PaLD distinguishes itself relative to knn and the unsupervised algorithms studied in [9].

<sup>6</sup>Note that, without speed up, thoroughly evaluating a benchmark with over two thousand data points is impractical; see, for comparison, Table 1.

<sup>7</sup>A related option, for example, would be to consider data labeled as anomalies in a more semi-supervised fashion.

We observe differing performance for knn and PaLD with each beating out the other 4 out of 8 times. For knn, we observe perfect scores for Lymphography and WBC, consistent with low numbers of anomalies (6 and 10, respectively) to successfully detect<sup>8</sup>. For the 4 out of 8 times when PaLD is less performant, the difference is relatively modest.

Interestingly, PaLD

- outperforms all 14 unsupervised benchmarks from [9] 3 out of 8 times and;
- exhibits a worst-case ROC AUC of over 60%,

indicating an ability to be at least somewhat informative in a variety of conditions. Further study of PaLD-based anomaly detection against a broader array of challenging benchmarks would be needed to characterize performance as well as consideration of robustness to our choice of PaLD-based anomaly detection test statistic.

TABLE 3

*Anomaly detection results for 8 healthcare benchmarks for area under curve (AUC) metrics for the receiving operator characteristic (ROC) and precision recall (PR) curves. Cases where the best performance by an unsupervised algorithm reported in [9] is met or exceeded by PaLD are underlined.*

Dataset	knn		PaLD		Best Unsupervised in [9]	
	ROC	PR	ROC	PR	ROC	PR
breastw	<b>99.6</b>	<b>99.1</b>	96.9	93.3	99.7	99.4
cardio	90.0	55.8	<b>95.9</b>	<b>69.4</b>	<u>95.6</u>	<u>68.4</u>
Cardiotocography	78.1	50.8	<b>84.3</b>	<b>63.0</b>	<u>77.8</u>	<u>52.6</u>
Hepatitis	55.0	0.28	<b>63.8</b>	<b>34.5</b>	82.0	41.5
Lymphography	<b>1.0</b>	<b>1.0</b>	94.2	41.2	99.8	97.6
Pima	<b>68.5</b>	<b>58.0</b>	65.0	51.5	73.4	56.6
vertebral	27.7	9.1	<b>62.2</b>	<b>18.4</b>	<u>53.2</u>	<u>15.2</u>
WBC	<b>1.0</b>	<b>1.0</b>	94.8	48.0	99.5	92.3

**3.2. Semi-supervised prediction.** As an application of semi-supervised prediction, we consider a dataset from a recent benchmark [18] for network neuroscience with  $n = 195$  and  $d = 4950$ . The Parkinson’s Progression Markers Initiative (PPMI) dataset labels each subject with 4 clinically relevant classes: normal control, scans without evidence of dopaminergic deficit (SWEDD), prodromal, and Parkinson’s disease (PD). These ordinal classes correspond to increasingly severe biomarkers. On a practical level, low  $n$  is driven by the cost to obtain labels while high  $d$  is due to that fact that the matrix of correlations that quantifies a brain network (one per subject) scales quadratically in the number of regions of interest (ROIs) for the brain atlas employed to aggregate voxels from brain scan measurements. For the present illustration, we consider the Schafer atlas with 100 ROIs, a standard atlas that performs well across many benchmarks in [18], including PPMI.

**Experimental design.** The present illustration explores classification via online PaLD as compared to knn by holding reference data for evaluation. Specifically, we use 10 folds to make rough comparisons to the accuracy result reported [18] possible<sup>9</sup> so that, after randomization<sup>10</sup>, we have 10 test units, each of which trains on 9 out of 10 folds and evaluates accuracy on the remaining 10 percent of the data. As a result, each labeled correlation matrix in the PPMI benchmark is classified one time.

<sup>8</sup>For comparison, ROC AUC values of 55.9 and 90.6 for Lymphography and WBC, respectively, appear in [9, Table D4] for the knn parameter selections (and randomizations) made there.

<sup>9</sup>For simplicity, we do not explore parameter tuning, as is done in [18].

<sup>10</sup>A stratified shuffle of the data is employed to balance the distribution of labels across folds and the same shuffle is employed across the algorithms evaluated.

An example test unit might have 176 reference data  $S$  with 19 labeled correlation matrices  $t$  held out to the evaluate accuracy of online prediction.

Following [14], we consider 6 different classification methods derived from the cohesion matrix of the reference data  $S$  plus one test point  $t$ ; recall  $T = S \cup \{t\}$ . All six methods measure how strongly  $t$  is associated with each of the 4 classes  $S_i$  within the labeled data  $S$ . The class with the strongest association metric is selected to classify the test point  $t$ : greater values are stronger.

Four methods are based on aggregating information over the neighborhood of  $t$ , similar to knn. Two Count metrics consider how many cohesion values exceed the natural threshold  $\tau(T, d)$  with

$$(3.2) \quad \nu_i(t) \stackrel{\text{def}}{=} \sum_{x \in S_i} I(c_{x,t} \geq \tau(T, d))$$

based on the cohesion to class  $S_i$  where  $I(c_{x,t} \geq \tau(T, d))$  is a 0/1 indicator. A Count metric for the number of strong cohesion values from the each class is defined analogously. Two Sum methods are based on adding the cohesion values that exceed the natural threshold with

$$(3.3) \quad \sigma_i(t) \stackrel{\text{def}}{=} \sum_{x \in S_i} I(c_{x,t} \geq \tau(T, d)) \cdot c_{x,t}$$

based on the cohesion to class  $S_i$ ; a Sum method for strong cohesion from each class is defined analogously.

Similar to  $a(t)$  defined above (3.1), two methods consider maximal cohesion to and from each class. One Max metric is based on cohesion to each class

$$(3.4) \quad \mu_i(t) \stackrel{\text{def}}{=} \max_{x \in S_i} c_{x,t};$$

a Max metric for the maximal cohesion from each class is defined analogously. See [14] for further discussion.

As in the previous subsection, we do not evaluate the precise reduction in computational time obtained by using online PaLD, which scales with the size of the training data, since we want to take advantage of the greater than  $10^2$  speed up. See subsection 2.3 for speed up validation.

TABLE 4

*Mean accuracy across ten folds ( $\pm$  one standard deviation) for six cohesion-based classifiers described by (3.2), (3.3), and (3.4) as compared to knn for the PPMI dataset with the Schafer atlas.*

Cohesion To			Cohesion From			knn
Count	Sum	Max	Count	Sum	Max	
$0.59 \pm 0.05$	$0.59 \pm 0.06$	$0.49 \pm 0.1$	$0.59 \pm 0.04$	$0.57 \pm 0.04$	$0.49 \pm 0.09$	$0.57 \pm 0.07$

**Results.** For this initial experimentation, we observe that the two methods using a max cohesion value underperform knn, but the 4 classifiers aggregating over the neighborhood of the test point narrowly outperform knn. The 4 strong neighborhood classifiers may even provide lower variation in predictive accuracy as compared knn, but this hypothesis would warrant broader study across benchmarks.

These results are in the general range of accuracy results reported in [18] where the mean accuracy for PPMI with the Schafer atlas lies within [56.5, 63.2] for conventional machine learning methods. We caution the reader not to place too much

weight on these baseline results for the PPMI benchmark since they do not exploit network structure nor do they systematically address the potential for variation in the measurement process to obtain a correlation matrix for each subject<sup>11</sup>. There is much to explore for this benchmark and consideration of PaLD-based classification increases the potential dimensions to explore further.

The first exploration we pursued was testing the sensitivity of the results to the randomization of the reference data. That is, if we re-ran the entire experiment, how much variation in the reported mean accuracy should be expected for a given method? By sampling 10 seeds for randomization, we observed mean accuracies of  $0.60 \pm 0.01$  (resp.,  $0.48 \pm 0.03$ ) for the count of strong ties to class  $i$  (resp., max cohesion to class  $i$ ) method where  $\pm\sigma$  reports the standard deviation of the mean accuracy for each point being tested once, under the random shuffle for a given seed. Each sensitivity statistic takes around 220 sec to compute as compared to about 10 hours that would be needed by the original PaLD implementation based on complexity projections.

**4. Discussion.** Online PaLD presents intriguing possibilities for further investigation. By making datasets with  $n = 10^5$  accessible with straightforward training, PaLD’s potential to be further explored prior to bringing in approximations is increased. For instance, investigating AD bench [9] for datasets with  $n < 7000$ —including a cross section of computer vision and natural language processing benchmarks introduced in [9]—could proceed before bringing in approximation techniques to complete the analysis, up to  $n = 619326$ .

Exact PaLD, with its theoretical guarantees, may be attractive to avoid any uncertainty being introduced via approximation, especially for situations where reference data is carefully maintained and not too large. For example, the THINGS initiative (<https://things-initiative.org/>) developed 1,854 object concepts and curated reference data (such as 26,107 high quality images manually associated to concepts [11]). Whereas the original work on PaLD [5] might provide an interesting unsupervised analysis of these concepts (see [10] for comparison), online PaLD is adapted to associate “test” concepts (e.g., from user input or some machine interface) to the THINGS reference data. Comparisons to reference images invite combining the ideas in this article with principled approximation techniques [1] or computer science approaches [6, 14] to make such comparisons readily accessible.

As a novel approach to anomaly detection and semi-supervised classification, PaLD is relatively unexplored. Though not explored here, an intriguing possibility is to combine semi-supervised classification with anomaly detection such that any test point deemed too distant from the training data would simply not be classified. A key question to investigate is how much excluding anomalous test points might increase predictive accuracy. As above, a natural point of comparison would be to  $k$ -nearest neighbors, which applies to both semi-supervised classification and anomaly detection.

**Conclusions.** We demonstrated how the partitioned local depth framework can be adapted to online applications. By analyzing the original, exact algorithm, we limit the complexity of analyzing a test point  $t$  relative to reference data  $S$ . Our illustrations with health care data show the potential to apply online PaLD to applications where an alternative to the  $k$ -nearest neighbor algorithm is desired. The online point-of-view we presented complements principled approximation techniques [1] and computer

---

<sup>11</sup>There may even be some value in PaLD processing of correlations between ROIs to absorb some of this variation.

science approaches [6, 14], inviting future work to hybridize these ideas to study large datasets. More immediately, online PaLD can help accelerate experimentation across datasets and algorithmic approaches for online applications.

**Acknowledgments.** We would like to acknowledge helpful discussion of this article with Kenneth Berenhaut and the Metron fellows.

### References.

- [1] J. D. BARON, R. DARLING, J. L. DAVIS, AND R. PETTIT, *Partitioned k-nearest neighbor local depth for scalable comparison-based learning*, Preprint, (2021), p. 27. Available at: arXiv:2108.08864.
- [2] K. S. BERENHAUT, J. D. FOLEY, AND L. LYU, *Generalized partitioned local depth*, Journal of Statistical Theory and Practice, 18 (2024), p. 17, <https://doi.org/10.1007/s42519-023-00356-1>.
- [3] K. S. BERENHAUT, L. LTU, AND Y. ZHOU, *Bonded and dissipative connections in the context of communities and cohesion*, 2025. In revision.
- [4] K. S. BERENHAUT AND K. E. MOORE, *Communities in data*, SIAM News, (2022).
- [5] K. S. BERENHAUT, K. E. MOORE, AND R. L. MELVIN, *A social perspective on perceived distances reveals deep community structures*, Proceedings of the National Academy of Sciences, 119 (2022), p. e2003634119, <https://doi.org/10.1073/pnas.2003634119>.
- [6] A. DEVARAKONDA AND G. BALLARD, *Sequential and shared-memory parallel algorithms for partitioned local depths*, in Proceedings of the 2024 SIAM Conference on Parallel Processing for Scientific Computing (PP), SIAM, 2024, pp. 53–64.
- [7] C. EVANS AND K. S. BERENHAUT, *Two-sample testing with local community depth*, International Journal of Data Science and Analytics, (2024), pp. 1–20.
- [8] P. FRÄNTI AND S. SIERANOJA, *K-means properties on six clustering benchmark datasets*, Applied intelligence, 48 (2018), pp. 4743–4759.
- [9] S. HAN, X. HU, H. HUANG, M. JIANG, AND Y. ZHAO, *Adbench: Anomaly detection benchmark*, Advances in neural information processing systems, 35 (2022), pp. 32142–32159.
- [10] M. N. HEBART, O. CONTIER, L. TEICHMANN, A. H. ROCKTER, C. Y. ZHENG, A. KIDDER, A. CORRIVEAU, M. VAZIRI-PASHKAM, AND C. I. BAKER, *Things-data, a multimodal collection of large-scale datasets for investigating object representations in human brain and behavior*, Elife, 12 (2023), p. e82580.
- [11] M. N. HEBART, A. H. DICKTER, A. KIDDER, W. Y. KWOK, A. CORRIVEAU, C. VAN WICKLIN, AND C. I. BAKER, *Things: A database of 1,854 object concepts and more than 26,000 naturalistic object images*, PloS one, 14 (2019), p. e0223792.
- [12] M. G. KHOURY, K. S. BERENHAUT, K. E. MOORE, E. E. ALLEN, A. F. HARKEY, J. K. MUHLEMANN, C. N. CRAVEN, J. XU, S. S. JAIN, D. J. JOHN, ET AL., *Partitioned local depth analysis of time course transcriptomic data reveals elaborate community structure*, bioRxiv, (2022), pp. 2022–07.
- [13] M. G. KHOURY, K. S. BERENHAUT, K. E. MOORE, E. E. ALLEN, A. F. HARKEY, J. K. MÜHLEMANN, C. N. CRAVEN, J. XU, S. S. JAIN, D. J. JOHN, ET AL., *Informative community structure revealed using arabidopsis time series transcriptome data via partitioned local depth*, in silico Plants, 6 (2024), p. diad018.
- [14] R. LANGEFELD, *Employing partitioned local depth (pald) in a supervised learning context*, B. S. Thesis, Wake Forest University, (2024), p. 24.

- [15] L. D. McGOWAN, K. E. MOORE, AND K. S. BERENHAUT, *Partitioned local depth (pald) community analyses in r*, The R Journal, (2025). Accepted.
- [16] K. E. MOORE, *Mathematical foundations of data cohesion*, Preprint, (2023), p. 20. Available at: arXiv:2308.02546.
- [17] S. SIERANOJA AND P. FRÄNTI, *Fast and general density peaks clustering*, Pattern recognition letters, 128 (2019), pp. 551–558.
- [18] J. XU, Y. YANG, D. HUANG, S. S. GURURAJAPATHY, Y. KE, M. QIAO, A. WANG, H. KUMAR, J. MCGEOWN, AND E. KWON, *Data-driven network neuroscience: On data collection and benchmark*, Advances in Neural Information Processing Systems, 36 (2023), pp. 21841–21856.

**Appendix A. Derivations and detailed considerations.** This appendix includes a detailed derivation of the marginal formula for  $\tau(T, d)$  and a discussion of considerations to extend this derivation to the generalized PaLD framework [2]. We close with a discussion of the challenges inherent in maintaining a full cohesion network, which are elucidated by the preceding derivations.

**A.1. Derivation of the natural threshold formula.** Let us now derive a formula for  $\tau(T, d)$ . First, we note that:

$$(A.1) \quad 2n(n-1)\tau(S, d) = (n-1) \sum_{x \in S} c_{x,x} = \sum_{x \in S} \sum_{y \in S, y \neq x} \frac{I(x, x, y)}{|U_{x,y}^S|} = \sum_{x \in S} \sum_{y \in S, y \neq x} \frac{1}{|U_{x,y}^S|}$$

since, under our simplifying assumptions (2.9), the left equality follows from the formula for  $\tau(S, d)$  (2.6), the middle equality follows the explicit formula for cohesion (2.3) and  $I(x, x, y) = 1$  (rightmost equality). Similarly, we have that:

$$(A.2) \quad \begin{aligned} 2n(n+1)\tau(T, d) &= nc_{t,t}^T + n \sum_{x \in S} c_{x,x} = nc_{t,t}^T + \sum_{x \in S} \left( \frac{I(x, x, t)}{|U_{x,t}^T|} + \sum_{y \in S, y \neq x} \frac{I(x, x, y)}{|U_{x,y}^T|} \right) \\ &= nc_{t,t}^T + \sum_{x \in S} \left( \frac{1}{|U_{x,t}^T|} + \sum_{y \in S, y \neq x} \frac{1}{|U_{x,y}^T|} \right) \end{aligned}$$

by considering  $T$  in lieu of  $S$  and separating out quantities related to the test point  $t$ . Noting

$$(A.3) \quad \sum_{x \in S} \frac{1}{|U_{x,t}^T|} = \sum_{x \in S} \frac{1}{|U_{t,x}^T|} = nc_{t,t}^T,$$

we have:

$$(A.4) \quad 2n(n+1)\tau(T, d) = 2nc_{t,t}^T + \sum_{x \in S} \sum_{y \in S, y \neq x} \frac{1}{|U_{x,y}^T|}.$$

As we discussed during the derivation of Algorithm 2.3 in subsection 2.2 above, the set  $U_{x,y}^T$  can only differ from  $U_{x,y}^S$  by adding the element  $t$ , so:

$$(A.5) \quad \begin{aligned} \sum_{x \in S} \sum_{y \in S, y \neq x} \frac{1}{|U_{x,y}^T|} &= \sum_{x \in S} \sum_{y \in S, y \neq x} \frac{1}{|U_{x,y}^S|} - \left( \sum_{x \in S} \sum_{y \in S, y \neq x} \frac{I(t \in U_{x,y}^T)}{(|U_{x,y}^S| + 1)|U_{x,y}^S|} \right) \\ &= (n-1) \sum_{x \in S} c_{x,x}^S - \left( \sum_{x \in S} \sum_{y \in S, y \neq x} \frac{I(t \in U_{x,y}^T)}{(|U_{x,y}^S| + 1)|U_{x,y}^S|} \right) \end{aligned}$$

where  $I(t \in U_{x,y}^T)$  is an indicator of set membership and we can view the right most term  $\varepsilon(T, d)$  as a correction; see (2.12) for comparison. To summarize, we have that:

$$\begin{aligned} 2n(n+1)\tau(T, d) &= 2nc_{t,t}^T + \sum_{x \in S} \sum_{y \in S, y \neq x} \frac{1}{|U_{x,y}^T|} \\ (A.6) \quad &= 2nc_{t,t}^T + (n-1) \sum_{x \in S} c_{x,x}^S - \left( \sum_{x \in S} \sum_{y \in S, y \neq x} \frac{I(t \in U_{x,y}^T)}{(|U_{x,y}^S| + 1)|U_{x,y}^S|} \right) \end{aligned}$$

by considering the marginal impact adding  $t$  realized as (i) additional terms in summation formulae and (ii) increases in the size of some local foci. Upon division by  $2n(n+1)$ , the attractive marginal formula (2.11) is obtained.

**A.2. Considerations for an online algorithm for generalized PaLD.** The generalized partitioned local depth (GPaLD) framework extends PaLD to enable probabilistic consideration of uncertain, variable, and conflicting information [2]. For instance, GPaLD allows multiple dissimilarities to be combined using probabilistic weights. This potential to fuse disparate sources of information using the common currency of probability may be relevant to semi-supervised classification based on multiple types of predictor variables. Fortunately, the online algorithm presented is readily adapted to this more general context.

First, absent a notion of distance for GPaLD, we will define what we mean by the online setting in terms of the GPaLD concepts of local relevance and support division. Recall that the local relevance of  $z$  to the pair  $(x, y)$ , denoted  $R_{x,y,z}$  generalizes the notion of membership within the local focus  $z \in U_{x,y}$  to be, in general, a probability such that  $R_{x,y,z} = R_{y,x,z}$  and  $R_{x,y,x} = 1$  for all distinct  $x, y \in S$  and  $z \in S$ . The support division of  $z$  with respect the pair  $(x, y)$ , denoted  $Q_{x,y,z}$ , generalizes the indicator  $I(z, x, y)$  to be, in general, a probability distribution over  $\{Q_{x,y,z}, Q_{y,x,z}\}$  such that  $Q_{x,y,z} = 1 - Q_{y,x,z}$ . The online setting is concerned with extending the arrays and for distinct  $x, y \in S$  and  $z \in S$ , defined over the set  $S$ , to be defined over the set  $T = S \cup \{t\}$ .

For example, if multiple dissimilarities  $\{d_i\}_{i=1}^k$  are combined as in [2, 5.1], then extending this model to the test point  $t$  by testing  $k$  dissimilarities is consistent with this online setting. In essence, each  $d_i$  gets a (weighted) vote to combine local focus membership and support indicators probabilistically.

With these preliminaries, the natural threshold derivation is readily adapted. Our additional assumption that  $d(z, z) < d(z, y)$  becomes  $Q_{z,y,z} = 1$  (and hence,  $Q_{y,z,z} = 0$ ), which has the social interpretation that  $z$  fully supports itself. The observation that  $\tau(S, d)$  relates directly to the size of local foci (2.10) is replaced by the more general measure of the size  $V_{x,y}^S := \sum_{w \in S} R_{x,y,w}^S$ . The assumption of that  $R_{x,y,z} = R_{y,x,z}$  guarantees that  $V_{x,y}^S = V_{y,x}^S$  is a function of the set  $\{x, y\}$ . Likewise, the assumption that  $R_{x,y,x} = 1$  and  $Q_{x,y,x} = 1$  is analogous to  $I(x, x, y) = 1$  and we have:

$$(A.7) \quad 2n(n-1)\tau(S, \mathbf{R}, \mathbf{Q}) = \sum_{x \in S} \sum_{y \in S, y \neq x} \frac{1}{V_{x,y}^S}$$

Then, marginal analysis of the impact of extending  $\mathbf{R} = [R_{x,y,z}]$  and  $\mathbf{Q} = [Q_{x,y,z}]$  by a single  $t$  proceeds as in subsection A.1 and we update the marginal formula as follows:

$$(A.8) \quad \tau(T, \mathbf{R}, \mathbf{Q}) = \tau(S, \mathbf{R}, \mathbf{Q}) \frac{n-1}{n+1} + \frac{c_{t,t}^T}{n+1} - \varepsilon(T, \mathbf{R}, \mathbf{Q})$$

where  $V_{x,y}^T := V_{x,y}^S + R_{x,y,t}$ , by definition, and the right most correction term is

$$(A.9) \quad \varepsilon(T, \mathbf{R}, \mathbf{Q}) \stackrel{\text{def}}{=} \frac{1}{2n(n+1)} \sum_{x \in S} \sum_{y \in S, y \neq x} \frac{R_{x,y,t}}{(V_{x,y}^S + R_{x,y,t})V_{x,y}^S}.$$

**A.3. Challenges for maintaining a full cohesion network.** The derivations in the previous two subsections clarify the challenges in maintaining an exact cohesion network. In the above, we see that increases in the size of local foci can be handled systematically in  $O(n^2)$  time and, more generally, changes in local relevance are often tractable. For the special case of  $I(x, x, y)$ , our assumptions determine  $I(x, x, y) = 1$  and this makes determination of self-cohesion  $c_{x,x}$  and the threshold  $\tau(T, d)$  tractable.

However, support indicators  $I(x, w, y)$ , and support division more generally, are determined by triples of points. Thus, determination of the full cohesion network entails additional computation: for  $x \in S$  updating and may require  $O(n^2)$  steps. In essence, to determine  $c_{x,y}^T$  for  $x \neq y \in S$ , the division of support due to  $t$  must be determined. That is, extending the network requires determining  $I(t, x, y)$  whenever  $t \in U_{x,y}^T$ .

These considerations suggest lazy computation of  $c_{x,y}$  and introducing principled approximation techniques [1]. For example, one could consider setting  $I(t, x, y) := 1/2$  for  $|U_{x,y}^T| > \sqrt{n}$  and analyze how closely this approximates the exact determination of  $I(t, x, y)$ . It would be interesting to compare this simplistic proposal to the methods of [1] with  $k \approx \sqrt{n}$ . Such approaches take advantage of the fact that when the local focus  $U_{x,y}$  is large, many comparisons may be needed to determine cohesion exactly, but the corresponding contributions to cohesion are small.